Slow light effect via Rayleigh Anomaly and the effect of finite gratings

KYOUNG-YOUM KIM[1,2], XINYUAN CHONG[1], FANGHUI REN[1], AND ALAN X. WANG[1,*]

[1]*School of Electrical Engineering and Computer Science, Oregon State University, Corvallis, OR, USA, 97331*
[2]*Department of Electrical Engineering, Sejong University, Seoul 05006, South Korea*
**Corresponding author: wang@eecs.oregonstate.edu*

Received XX Month XXXX; revised XX Month, XXXX; accepted XX Month XXXX; posted XX Month XXXX (Doc. ID XXXXX); published XX Month XXXX

In this letter, we investigate slow light effect of subwavelength diffraction gratings via Rayleigh Anomaly using a fully analytical approach without the necessity to consider specific grating structures. Our results show that the local group velocity of the transmitted light can be significantly reduced due to the optical vortex, which can inspire a new mechanism to enhance light-matter interactions for optical sensing and photo detection. However, the slow light effect will diminish as the transmitted light propagates further away from the grating surface, and the slow-down factor decreases as the grating size shrinks. © 2015 Optical Society of America

OCIS codes: *(050.1950) Diffraction gratings; (050.6624) Subwavelength structures; (260.2110) Electromagnetic optics.*

http://dx.doi.org/10.1364/OL.99.099999

Diffraction gratings change the direction of incoming light [1]. Rayleigh Anomaly (sometimes called as Wood or Rayleigh-Wood Anomaly) indicates the phenomenon when diffracted lights are directed perpendicular to the surface normal of the grating [2-4]. Recently, it has attracted strong research interest due to its interplay with surface plasmon polariton (SPP) waves [5-13]. Applications such as extra-ordinary transmission (EOT) [11] and high-sensitivity optical sensors [9] have already been proposed and demonstrated. The interaction between SPP waves and Rayleigh Anomaly will result in highly localized optical field that is determined by the decaying SPP waves, typically on the order of one wavelength. Interestingly, people find that Rayleigh Anomaly alone can exhibit unique characteristics that are distinctively different from SPP waves. In this Letter, we explicitly point out that Rayleigh Anomaly can slow down the group velocity of the transmitted light, similar to the effect from photonic crystal waveguides [14] and plasmonic waveguide gratings [15]. And more importantly, this slow light effect can extend much further away from the grating surface than the SPP waves. This can, say, increase the interaction time between light and matter over a long path, and thus be applied to the realization of enhanced optical sensing or photo detection capabilities. However, we found that both the slow-down factor and the effective range depend on the grating size. Therefore, we further investigate the finite-size effect of gratings that is unavoidable in actual applications.

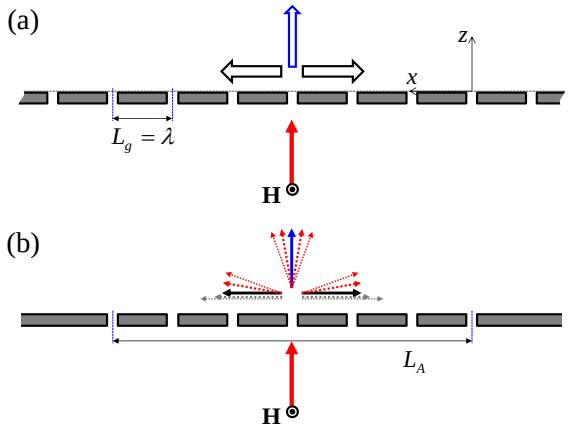

Fig. 1. Geometry of the (a) infinite and (b) finite gratings. L_g and L_A denote the grating period and the length of the finite grating, respectively. In (a), the transmitted light has only three wave vectors (see the blue and black unfilled arrows). However, the finite-size effect induces additional wave vectors around each of them [see the dotted red and gray arrows in (b) that correspond to propagating and evanescent diffracted waves, respectively].

We begin our discussion with the grating shown in Fig. 1(a). It has a period L_g and can be made of dielectrics or metals. If it is metallic, we assume further that it is not thick enough for the perforations between metallic grooves to guide SPP waves along the z direction. Since our target applications are sensors utilizing the enhanced interaction between slow light and objects in free space, we limit our attention to the transmission-type grating. A TM-polarized light, propagating in the $+z$ direction, is assumed to be normally incident to this grating. Since the grating is periodic infinitely, the magnetic field distribution at its exit plane (taken as $z = 0$) can be expanded as

$$\mathbf{H}_I(x,0) = \hat{\mathbf{y}} \sum_{n=-\infty}^{\infty} a_n e^{jn\Lambda x}, \qquad \textbf{(1)}$$

where $\Lambda = 2\pi / L_g$. a_n represents the amplitude of the n-th harmonic field component that can be easily obtained by either the finite element method (FEM) or the rigorous coupled wave analysis (RCWA).

Using the angular spectrum expansion [1], the magnetic field of the transmitted light in $z>0$ can be written as

$$\mathbf{H}_I = \hat{\mathbf{y}} \sum_{n=-\infty}^{\infty} a_n e^{j(n\Lambda x + \sqrt{k_0^2 - (n\Lambda)^2} z)}, \quad \textbf{(2)}$$

where $k_0 = 2\pi/\lambda$ and λ is the wavelength of light in free space. Rayleigh Anomaly occurs when $\Lambda \approx k_0$ or $L_g \approx \lambda$, resulting in [16]

$$\mathbf{H}_I = \hat{\mathbf{y}}[a_0 e^{jk_0 z} + 2a_1 \cos(k_0 x)], \quad \textbf{(3)}$$

where we considered only the first-order diffraction. For the simplicity of discussion, we also assumed that the grating structure (e.g., its permittivity distribution) is symmetric with respect to the z axis, which makes a_1 real. The second term on the right side of Eq. (3) shows that diffracted lights have no wave vector components in the z direction and form a kind of standing wave in the x direction.

Using Eq. (3), we can easily derive

$$\tilde{S}_x = 2|a_0 a_1| \sin(k_0 x) \sin(k_0 z + \angle a_0 a_1), \quad \textbf{(4)}$$

$$\tilde{S}_z = |a_0|^2 + 2|a_0 a_1| \cos(k_0 x) \cos(k_0 z + \angle a_0 a_1), \quad \textbf{(5)}$$

$$\tilde{w} = |a_0|^2 + 2|a_1|^2 + 2|a_0 a_1| \cos(k_0 x) \cos(k_0 z + \angle a_0 a_1), \quad \textbf{(6)}$$

where $\mathbf{S} = (\eta_0/2)(\tilde{S}_x, \tilde{S}_z)$ and $w = (\mu_0/2)\tilde{w}$ denote the Poynting vector and energy density of the transmitted light, respectively. η_0 and μ_0 are the impedance and permeability of free space, and their quotient becomes the speed of light in free space ($c = \eta_0/\mu_0$). The energy velocity of light can be obtained by $\mathbf{v} = \mathbf{S}/w$ [17], resulting in

$$v_z(x, z>0) = c\left(1 - \frac{2|a_1|^2}{\tilde{w}}\right). \quad \textbf{(7)}$$

It is well-known that this velocity coincides with the group velocity of light in free space [18-20]. Equation (7) shows that the amount of velocity reduction is determined by how much energy of the transmitted light is stored purely in the diffracted-wave components.

One more phenomenon to note is the so-called optical vortex [16,21-23]. Equations (4)-(5) show that the Poynting vector becomes zero at the points whose coordinates satisfy

$$2\cos(k_0 x)\cos(k_0 z + \angle a_0 a_1) = -|a_0|/|a_1|, \quad \textbf{(8)}$$

$$\sin(k_0 x)\sin(k_0 z + \angle a_0 a_1) = 0. \quad \textbf{(9)}$$

Because optical power cannot flow through these points, there occur optical vortices, a kind of detours around them. They increase the effective path length of the transmitted light and effectively reduce its velocity in the longitudinal direction. It is notable that such singular points and resultant vortices can appear only when $\eta = |a_1|/|a_0| \geq 0.5$ [see Eq. (8)].

To increase η, we had better use metallic gratings. In such cases, SPP waves can be launched and interfere with the transmitted light. Fortunately, their effect can be neglected because their contribution will be dominant only in a very near-field region ($z << \lambda$), and disappear in the region where our interest lies ($z >> \lambda$).

In Figs. 2(a)-2(b), we plotted the longitudinal velocity v_z of the transmitted light at x = 0, taking different values of η^2. They show clearly that the larger η^2 is, the slower the spatial average of v_z tends to be. Moreover, the vortex effect becomes effective when $\eta^2 \geq 0.25$, resulting in negative v_z [see Fig. 2(c) for an exemplary distribution of Poynting vectors when such vortices are formed through a metallic grating]. This can significantly slow down the average group velocity of the transmitted light. We note that the transverse velocity v_x is zero at $x = m(\lambda/2)$ [where m is an integer; see Eq. (4)]. This is because the grating generates two counter-propagating lights that can produce standing waves in the transverse direction. These characteristics reveal that Rayleigh Anomaly can be used to slow down light in free space. And ideally, the optical field pattern of the transmitted light will repeat itself with period of λ along the z direction, which indicates infinitely long effective range for slow light.

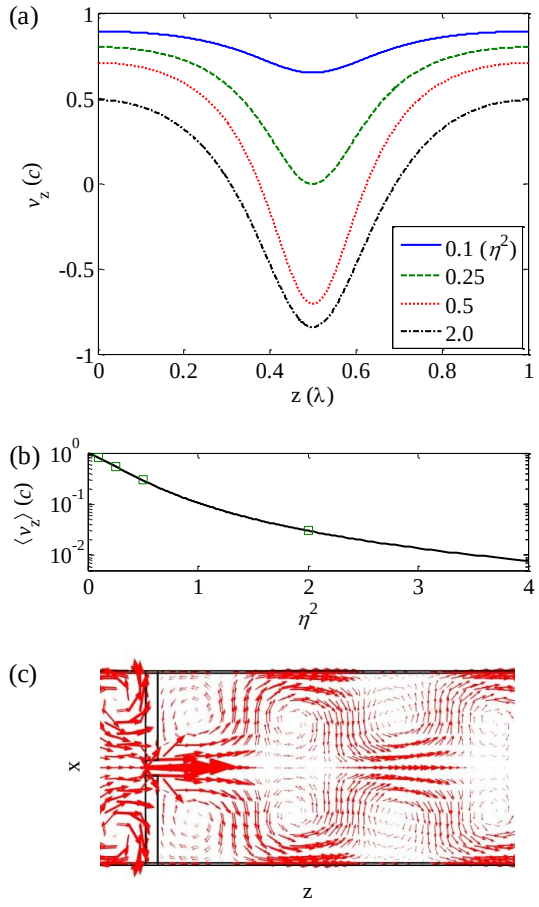

Fig. 2. (a) Longitudinal velocity (v_z) of the transmitted light at x = 0. Since the grating is assumed to be infinite, v_z becomes periodic in the z direction. (b) Spatial average of v_z ($\langle v_z \rangle$) over one wavelength along the z direction. It becomes 0.80c, 0.55c, 0.29c, and 0.03c (see the squares) when η^2 is 0.1, 0.25, 0.5, and 2.0, respectively. (c) An exemplary distribution of Poynting vectors, exhibiting optical vortices.

However, in actual applications, the grating size is always finite. However, to take this 'finiteness' into account is quite troublesome. If we use RCWA methods, we always come to impose a periodicity on the grating. FEM calculations can be useful but if the grating size is quite large (but finite), heavy computer resources and high calculation times are required. There are a few semi-analytic methods that basically treat the finite grating as an array of electromagnetic radiators or scatters [24-26]. However, they are somewhat too complicated and are not adequate for gratings with more than ~ 10^3 periods. Hereafter, we will develop a simple way of dealing with finite gratings, and investigate how their 'finiteness' affects on the slowdown factor and slow light effective range via Rayleigh Anomaly.

Let us see Fig. 1(b) where we depicted a finite size grating with a length of L_A. In this case, the magnetic field distribution at the exit plane will be no longer periodic. Therefore, we have instead of Eq. (1)

$$\mathbf{H}_F(x,0) = \hat{\mathbf{y}}\frac{1}{2\pi}\int T(k_x)e^{jk_x x}dk_x, \quad \textbf{(10)}$$

where $T(k_x)$ is the Fourier transform (FT) of $\mathbf{H}_F(x,0)\cdot\hat{\mathbf{y}}$. Since we can presume $\mathbf{H}_F(x,0)\cdot\hat{\mathbf{y}} = (\mathbf{H}_I(x,0)\cdot\hat{\mathbf{y}})\mathrm{rect}(x/L_A)$, $T(k_x)$ can be calculated by the convolution of the FT of $\mathbf{H}_I(x,0)\cdot\hat{\mathbf{y}}$ and that of $\mathrm{rect}(x/L_A)$, i.e., $L_A\mathrm{sinc}(L_A k_x/2\pi)$. Using Eq. (1), we can write the FT of $\mathbf{H}_I(x,0)\cdot\hat{\mathbf{y}}$ as $2\pi\sum_n a_n\delta(k_x - n\Lambda)$, which entails

$$T(k_x) = L_A\sum_n a_n \mathrm{sinc}\left(\frac{L_A(k_x - nk_0)}{2\pi}\right). \quad \textbf{(11)}$$

To take only the first-order diffraction into account, we need to consider just three terms of this summation corresponding to n = -1 to 1. Then, we have

$$\begin{aligned}\mathbf{H}_F = \hat{\mathbf{y}}\frac{L_A}{2\pi}\Bigg[& a_0\int \mathrm{sinc}\left(\frac{L_A k_x}{2\pi}\right)e^{jk_x x}e^{j\sqrt{k_0^2-k_x^2}z}dk_x \\ & + a_1\int \mathrm{sinc}\left(\frac{L_A k_x}{2\pi}\right)e^{j(k_x+k_0)x}e^{j\sqrt{k_0^2-(k_x+k_0)^2}z}dk_x \\ & + a_1\int \mathrm{sinc}\left(\frac{L_A k_x}{2\pi}\right)e^{j(k_x-k_0)x}e^{j\sqrt{k_0^2-(k_x-k_0)^2}z}dk_x\Bigg].\end{aligned} \quad \textbf{(12)}$$

We can further approximate Eq. (12) by changing each integral into a summation over an integer n with the substitution of $k_x = (n\Delta)k_0$. Fortunately, we do not need to consider large values of k_x (or $n\Delta$) because the sinc function becomes negligible for them. Let us define $n_{\max}$ as the maximum value of n. Then, the maximum argument of the sinc function becomes $n_{\max}\Delta N_g$ where $N_g = L_A/L_g$ (the number of periods in the finite grating). If we want to take into account up to M side lobes of the sinc function, we can put $n_{\max}\Delta N_g = M$. This entails $n_{\max}\Delta = M/N_g << 1$ since 3 or 4 is enough for M. We can thus use $\sqrt{k_0^2-k_x^2} = k_0\sqrt{1-(n\Delta)^2} \approx k_0$ and $\sqrt{k_0^2-(k_x \mp k_0)^2} \approx k_0\sqrt{\pm 2n\Delta}$.

After some algebra with these approximations, we can finally obtain

$$\begin{aligned}\mathbf{H}_F = \hat{\mathbf{y}}\Big[& a_0' e^{jk_0 z} + 2\sum_{n=1}^{n_{\max}}\chi_{0n}\cos(n\Delta k_0 x)e^{jk_0 z} \\ & + 2a_1'\cos(k_0 x) + 2\sum_{\substack{n=-n_{\max}\\ n\neq 0}}^{n_{\max}}\chi_{1n}\cos[(1-n\Delta)k_0 x]e^{j\sqrt{2n\Delta}k_0 z}\Big],\end{aligned} \quad \textbf{(13)}$$

where $a_{0(1)}' = (\Delta N_g)a_{0(1)}$ and $\chi_{0(1)n} = a_{0(1)}'\mathrm{sinc}(n\Delta N_g)$. Let us compare Eq. (13) with Eq. (3). In the case of an infinite grating, the transmitted light has only three wave vectors: $\mathbf{k}_0 = k_0(0,1)$ and $\mathbf{k}_{\pm 1} = k_0(\pm 1, 0)$. However, the 'finiteness' of the grating brings forth additional wave vectors *around* each of them as is schematically shown in Fig. 1(b): $\mathbf{k}_0^{(n)} = k_0(n\Delta, 1)$ and $\mathbf{k}_{\pm 1}^{(n)} = k_0(\pm(1-n\Delta), \sqrt{2n\Delta})$. We should point out that while all of $\mathbf{k}_0^{(n)}$ are real vectors, i.e., they all imply propagating diffracted waves, half of $\mathbf{k}_{\pm 1}^{(n)}$ (with n < 0) correspond to evanescent diffracted waves.

Equation (13) results in

$$v_z(x, z>0) = c\left(1 - \frac{2\Theta}{\tilde{w}}\right), \quad \textbf{(14)}$$

where $\Theta = \Theta_{pr} + \Theta_{ev}$. Θ_{pr} and Θ_{ev} are related to the amounts of velocity reduction due to the propagating and evanescent diffracted waves, respectively [see the fourth term of the right side of Eq. (13)], and are given by

$$\begin{aligned}\Theta_{pr} = & |a_1'|^2 + \sum_{n>0}|\chi_{1n}|^2 + 2\sum_{n>0}|a_1'\chi_{1n}|\cos(n\Delta k_0 x) \\ & \times\cos(\sqrt{2n\Delta}k_0 z) + 2\sum_{n>0}\sum_{m>n}|\chi_{1n}\chi_{1m}|\cos[(m-n)\Delta k_0 x] \\ & \times\cos[(\sqrt{2n\Delta}-\sqrt{2m\Delta})k_0 z],\end{aligned} \quad \textbf{(15)}$$

$$\begin{aligned}\Theta_{ev} = & \sum_{n<0}|\chi_{1n}|^2 e^{-2\sqrt{2|n|\Delta}k_0 z} + 2\sum_{n<0}|a_1'\chi_{1n}|e^{-\sqrt{2|n|\Delta}k_0 z} \\ & \times\cos(n\Delta k_0 x) + 2\sum_{\substack{n<0\\ m\neq 0}}^{m>n}\sum|\chi_{1n}\chi_{1m}|e^{-(\sqrt{2|n|\Delta}+\mathrm{Im}\{\sqrt{2m\Delta}\})k_0 z} \\ & \times\cos[(m-n)\Delta k_0 x]\cos(\sqrt{2m\Delta}k_0 z).\end{aligned} \quad \textbf{(16)}$$

The above results show that for our analysis of a finite grating, just the values of a_0 and a_1 that the finite grating would have if its size becomes infinite are required. We must point out that no further details of the grating structure such as adopted materials or geometry are necessary in our analytical approach. This is an advantage in that these results can be applied to a wide range of gratings.

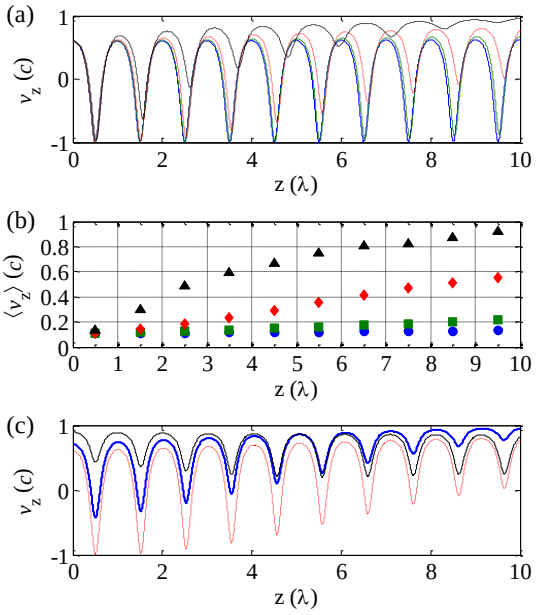

Fig. 3. Finite-size effect of the grating on (a) v_z and (b) $\langle v_z \rangle$ at x = 0. Solid, dashed, dotted, and dash-dotted lines in (a) and circles, squares, diamonds, and triangles in (b) correspond to N_g = 10^5, 10^4, 10^3, and 10^2, respectively. (c) Values of $v_z(0,z)$ with $\Theta = \Theta_{pr}$ (thin solid) and $\Theta = \Theta_{ev}$ (thick solid) when N_g = 10^3. The dotted line corresponds to $\Theta = \Theta_{pr} + \Theta_{ev}$ shown in (a).

Now, let us observe the finite-size effect numerically. In Figs. 3(a)-3(b), we compared the longitudinal velocities of the transmitted light through finite gratings of different lengths. We set x = 0 and assumed the same grating structure so that a_0, a_1, and η remain the same in all cases ($\eta^2 = 1$). The results show that a smaller N_g makes the vortex effect vanish after some propagation distance [see Fig. 3(a)], as a result of which the spatial average of v_z increases as the transmitted light propagates further away from the grating [see Fig. 3(b)]. To examine

this further, we calculated $v_z(0,z)$ with $\Theta = \Theta_{pr}$ (neglecting Θ_{ev}) and vice versa, and plotted the results in Fig. 3(c) (when N_g =10^3). The figure clearly demonstrates that such waning of the 'slow-down' feature via Rayleigh Anomaly results mostly from Θ_{ev} or the contribution of evanescent diffracted waves.

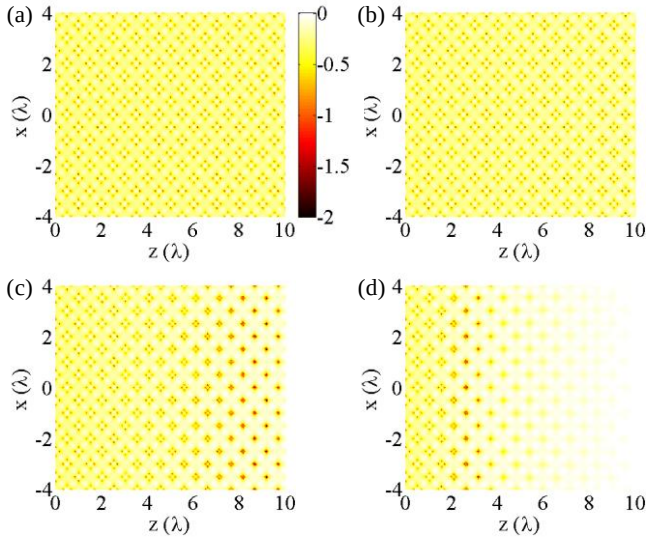

Fig. 4. Finite-size effect of the grating on the speed of the transmitted light, $|\mathbf{v}|(x,z)$. (a)-(d) correspond to the cases of N_g = 10^5, 10^4, 10^3, and 10^2, respectively. Please note that we have plotted the logarithmic values of the speed, i.e., $\log_{10}(|\mathbf{v}|/c)$, setting its minimum to be -2.

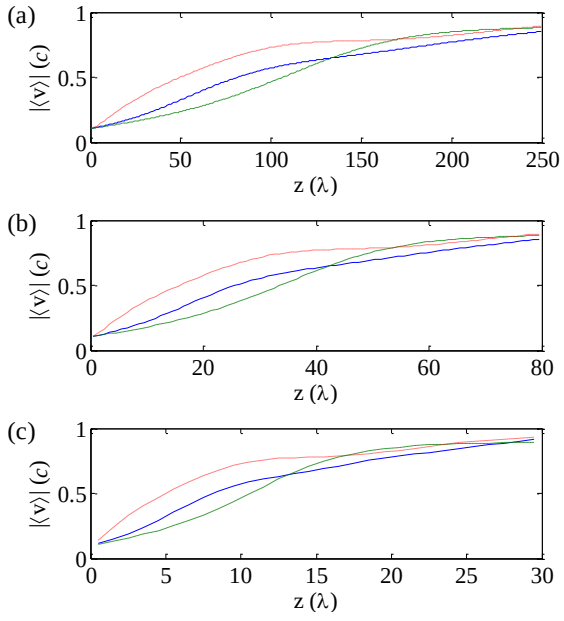

Fig. 5. Spatial average of the speed ($|\mathbf{v}|$) of the transmitted light when N_g is (a) 10^5, (b) 10^4, and (c) 10^3. Solid, dashed, and dotted lines in each figure correspond to $|\mathbf{v}|(0,z)$, $|\mathbf{v}|(0.2N_g,z)$, and $|\mathbf{v}|(0.4N_g,z)$, respectively.

Contrary to the infinite grating case, the grating geometry is not symmetric with respect to the translation in the *x* direction. This makes v_x not vanish even at $x = m(\lambda/2)$ (except for $m = 0$). We thus showed the logarithmic values of $|\mathbf{v}|$, i.e., the speed of the transmitted light in Fig. 4. The results exhibit that the 'slow-down' characteristics via Rayleigh Anomaly can be implemented at not only on-axis but also off-axis points. In Fig. 5, we further plotted the spatial average values of $|\mathbf{v}|$ at $x = 0.2N_g$ and $0.4N_g$, comparing with those at the on-axis points. It is quite evident from the figures that the variations in the speed of light (along both the *x* and *z* directions) become more noticeable when the grating size gets shorter. In many practical applications, it is very important to reduce the device size. Our analytic approach can be very useful from this point of view in that it can determine how far we can reduce the grating size while retaining the required characteristics.

In summary, we have developed a general analytical approach to investigate the slow light effect of Rayleigh Anomaly on diffraction gratings with both infinite and finite sizes. Our study shows that Rayleigh Anomaly can slow down the group velocities of the transmitted light over a very long effective range, but the effect will diminish as the size of the grating shrinks. This phenomenon suggests a new mechanism to improve the light matter interaction that can enhance the capabilities of optical sensing and photo detection.

National Science Foundation (NSF) (1342318) & National Institute of Health (NIH) (9R42ES024023).

References

1. J. Goodman, *Introduction to Fourier Optics* (McGraw-Hill, New York, 1996, 2nd ed.).
2. R. W. Wood, Phys. Rev. **48**, 928 (1935).
3. J. W. S. Rayleigh, Philos. Mag. **14**, 60 (1907).
4. U. Fano, J. Opt. Soc. Am. **31**, 213 (1941).
5. R. C. McPhedran and D. Maystre, Opt. Acta **21**, 413 (1974).
6. M. Sarrazin, J.-P. Vigneron, and J.-M. Vigoureux, Phys. Rev. B **67**, 085415 (2003).
7. J. M. Steele, C. E. Moran, A. Lee, C. M. Aguirre, and N. J. Halas, Phys. Rev. B **68**, 205103 (2003).
8. A. Christ, T. Zentgraf, J. Kuhl, S. G. Tikhodeev, N. A. Gippius, and H. Giessen, Phys. Rev. B **70**, 125113 (2004).
9. J. M. McMahon, J. Henzie, T. W. Odom, G. C. Schatz, and S. K. Gray, Opt. Express **15**, 18119 (2007).
10. H. Gao, J. M. McMahon, M. H. Lee, J. Henzie, S. K. Gray, G. C. Schatz, and T. W. Odom, Opt. Express. **17,** 2334 (2009).
11. Y.-W. Jiang, L. D.-C. Tzuang, Y.-H. Ye, Y.-T. Wu, M.-W. Tsai, C.-Y. Chen, and S.-C. Lee, Opt. Express **17**, 2631 (2009).
12. C.-Y. Lin, X. Wang, S. Chakravarty, B. S. Lee, W. Lai, J. Luo, A. K.-Y. Jen, and R. T. Chen, Appl. Phys. Lett. **97**, 093304 (2010).
13. Q. Gan, Z. Fu, Y. J. Ding, and F. J. Bartoli, Phys. Rev. Lett. **100**, 256803 (2008).
14. B. Luk'yanchuk, N. I. Zheludev, S. A. Maier, N. J. Halas, P. Nordlander, H. Giessen, and C. T. Chong, Nat. Materials **9**, 707 (2010).
15. F. Lopes-Tejeira, R. Paniagua-Dominguez, R. Rodriguez-Oliveros, and J. A. Sanchez-Jil, New J. Phys. **14**, 023035 (2012).
16. P. N. Stavrinou and L. Solymar, Opt. Commun. **206**, 217 (2002).
17. M. Born and E. Wolf, *Principles of Optics* (Cambridge University Press, Cambridge, 1999, 7th ed.).
18. L. J. F. Broer, Appl. Sci. Res. **A2**, 329 (1951).
19. M. A. Biot, Phys. Rev. **105**, 1129 (1957).
20. P. Y. Chen, R. C. McPhedran, C. M. de Sterke, C. G. Poulton, A. A. Asatryan, L. C. Botten, and M. J. Steel, Phys. Rev. A **82**, 053825 (2010).
21. E. Popov, L. Tsonev, and D. MayStre, J. Mod. Opt. **37**, 367 (1990).
22. A. A. Rizvi and C. H. Papas, Prog. Electromag. Res. PIER **29**, 261 (2000).
23. Y. Brûlé, G. Demésy, B. Gralak, and E. Popov, Opt. Express **23**, 9167 (2015).
24. D. M. Natarov, V. O. Byelobrov, R. Sauleau, T. M. Benson, and A. I. Nosich, Opt. Express **19**, 22176 (2011).
25. N. P. Stognii and N. K. Sakhnenko, IEEE J. Sel. Top. Quantum Electron. **19**, 4602207 (2013).
26. O. V. Shapovala and A. I. Nosich, AIP Advances **3**, 042120 (2013).

References with Titles

1. J. Goodman, *Introduction to Fourier Optics* (McGraw-Hill, New York, 1996, 2nd ed.).
2. R. W. Wood, "Anomalous diffraction gratings," Phys. Rev. **48**, 928-936 (1935).
3. J. W. S. Rayleigh, "Note on the remarkable case of diffraction spectra discovered by Prof. Wood," Philos. Mag. **14**, 60-65 (1907).
4. U. Fano, "The theory of anomalous diffraction gratings and of quasi-stationary waves on metallic surfaces (Sommerfeld's waves)," J. Opt. Soc. Am. **31**, 213-222 (1941).
5. R. C. McPhedran and D. Maystre, "A detailed theoretical study of the anomalies of a sinusoidal diffraction grating," Opt. Acta **21**, 413-421 (1974).
6. M. Sarrazin, J.-P. Vigneron, and J.-M. Vigoureux, "Role of Wood anomalies in optical properties of thin metallic films with a bidimensional array of subwavelength holes," Phys. Rev. B **67**, 085415 (2003).
7. J. M. Steele, C. E. Moran, A. Lee, C. M. Aguirre, and N. J. Halas, "Metallodielectric gratings with subwavelength slots: Optical properties," Phys. Rev. B **68**, 205103 (2003).
8. A. Christ, T. Zentgraf, J. Kuhl, S. G. Tikhodeev, N. A. Gippius, and H. Giessen, "Optical properties of planar metallic photonic crystal structures: Experiment and theory," Phys. Rev. B **70**, 125113 (2004).
9. J. M. McMahon, J. Henzie, T. W. Odom, G. C. Schatz, and S. K. Gray, "Tailoring the sensing capabilities of nanohole arrays in gold films with Rayleigh anomaly-surface plasmon polaritons," Opt. Express **15**, 18119-18129 (2007).
10. H. Gao, J. M. McMahon, M. H. Lee, J. Henzie, S. K. Gray, G. C. Schatz, and T. W. Odom, "Rayleigh anomaly-surface plasmon polariton resonances in palladium and gold subwavelength hole arrays," Opt. Express. **17,** 2334-2340 (2009).
11. Y.-W. Jiang, L. D.-C. Tzuang, Y.-H. Ye, Y.-T. Wu, M.-W. Tsai, C.-Y. Chen, and S.-C. Lee, "Effect of Wood's anomalies on the profile of extraordinary transmission spectra through metal periodic arrays of rectangular subwavelength holes with different aspect ratio," Opt. Express **17**, 2631–2637 (2009).
12. C.-Y. Lin, X. Wang, S. Chakravarty, B. S. Lee, W. Lai, J. Luo, A. K.-Y. Jen, and R. T. Chen, "Electro-optic polymer infiltrated silicon photonic crystal slot waveguide modulator with 23 dB slow light enhancement," Appl. Phys. Lett. **97**, 093304 (2010).
13. Q. Gan, Z. Fu, Y. J. Ding, and F. J. Bartoli, "Ultra-wide band slow light system based on THz plasmonic graded metal grating structures," Phys. Rev. Lett. **100**, 256803 (2008).
14. B. Luk'yanchuk, N. I. Zheludev, S. A. Maier, N. J. Halas, P. Nordlander, H. Giessen, and C. T. Chong, "The Fano resonance in plasmonic nanostructures and metamaterials," Nat. Materials **9**, 707-715 (2010).
15. F. Lopes-Tejeira, R. Paniagua-Dominguez, R. Rodriguez-Oliveros, and J. A. Sanchez-Jil, "Fano-like interference of plasmon resonances at a single rod-shaped nanoantenna," New J. Phys. **14**, 023035 (2012).
16. P. N. Stavrinou and L. Solymar, "The propagation of electromagnetic power through subwavelength slits in a metallic grating," Opt. Commun. **206**, 217-223 (2002).
17. M. Born and E. Wolf, *Principles of Optics* (Cambridge University Press, Cambridge, 1999, 7th ed.).
18. L. J. F. Broer, "On the propagation of energy in linear conservative waves," Appl. Sci. Res. **A2**, 329-344 (1951).
19. M. A. Biot, "General theorems on the equivalence of group velocity and energy transport," Phys. Rev. **105**, 1129-1137 (1957).
20. P. Y. Chen, R. C. McPhedran, C. M. de Sterke, C. G. Poulton, A. A. Asatryan, L. C. Botten, and M. J. Steel, "Group velocity in lossy periodic structured media," Phys. Rev. A **82**, 053825 (2010).
21. E. Popov, L. Tsonev, and D. MayStre, "Gratings-general properties of the Littrow mounting and energy flow distribution," J. Mod. Opt. **37**, 367–377 (1990).
22. A. A. Rizvi and C. H. Papas, "Power flow structures in two dimensional electromagnetic fields," Prog. Electromag. Res. PIER **29**, 261–294 (2000).
23. Y. Brûlé, G. Demésy, B. Gralak, and E. Popov, "Surface plasmon hurdles leading to a strongly localized giant field enhancement on two-dimensional (2D) metallic diffraction gratings," Opt. Express **23**, 9167-9182 (2015).
24. D. M. Natarov, V. O. Byelobrov, R. Sauleau, T. M. Benson, and A. I. Nosich, "Periodicity-induced effects in the scattering and absorption of light by infinite and finite gratings of circular silver nanowires," Opt. Express **19**, 22176-22190 (2011).
25. N. P. Stognii and N. K. Sakhnenko, "Plasmon resonances and their quality factors in a finite linear chain of coupled metal wires," IEEE J. Sel. Top. Quantum Electron. **19**, 4602207 (2013).
26. O. V. Shapovala and A. I. Nosich, "Finite gratings of many thin silver nanostrips: Optical resonances and role of periodicity," AIP Advances **3**, 042120 (2013).